SAND2007-6533C

Emissivity measurements of 3D photonic crystals at high temperatures

Ting Shan Luk[1], Timothy Mclellan[2], Ganesh Subramania[1], Jason C. Verley[1], and Ihab El-Kady[1]

[1] *Department of Photonics Microsystems Technologies, Sandia National Laboratories, Albuquerque, NM, USA*
[2] *Department of Electrical and Computer Engineering, University of New Mexico, Albuquerque, NM, USA*

Abstract

An accurate methodology is presented to measure photonic crystal emissivity using a direct method. This method addresses the issue of how to separate the emissions from the photonic crystal and the substrate. The method requires measuring two quantities: the total emissivity of the photonic crystal-substrate system, and the emissivity of the substrate alone. Our measurements have an uncertainty of 4% and represent the most accurate measure of a photonic crystal's emissivity. The measured results are compared to, and agree very well with, the independent emitter model.

Introduction:

The emittance of photonic crystals [1] has been a subject of intense study because of the potential use of photonic crystals as high temperature emitters for thermophotovoltaic applications [2, 3, 4]. This potential is due to the fact that photonic crystals are artificial materials with densities of states and spectral shapes that can be engineered. For an non-opaque objects, the "*extended*" Kirchhoff's law must be used to obtain the emissivity, e, such that $e = 1\text{-}R(\lambda)\text{-}T(\lambda)$, with $R(\lambda)$ and $T(\lambda)$ being the total reflectivity and transmissivity of the material, respectively. Theoretical predictions based on this approach are called indirect methods [5, 6]. In essence this approach calculates the effective absorptivity of the material that makes up the photonic crystal, convoluting it with the slow light effect of the photonic crystal, itself. This approach does not include the interplay between radiative and non-radiative relaxations of the emitters interacting with the electromagnetic fields inside the photonic crystal field. Alternatively, direct approaches based on quantum optics [7, 8], or stochastic Langevin electrodynamics [9, 10], do not assume an *a priori* maximum of 1 for the emissivity. None of these theoretical approaches consider the fact that photonic crystal often is built on a substrate and has finite number of periods. Therefore, theoretical transmittance and reflectance calculations are often for free-standing photonic crystals of infinite extent. Finally, the question remains whether the thermal excitation of a photonic crystal, with a strongly modified density of states, can be driven out of equilibrium; thus raising the possibility that the emissivity in a certain spectral range can exceed unity [3, 8, 7, 11, 12, 13, 14, 15].

Previous measurements performed on a tungsten photonic crystal in the temperature range of 404-546K [15] have shown that the emissivity is independent of temperature, and can be described *approximately* by $1\text{-}R(\lambda)$. The remaining small discrepancy was attributed to the use of specular reflectance for the $1\text{-}R(\lambda)$ calculation rather than, more correctly, the total reflectance. In these measurements, the transmittance of the photonic crystal-substrate system has not been properly accounted for because of the difficulty in measuring effective transmittance. In addition, the transmittance of the silicon substrate can change significantly with temperature along with resistivity, especially in the temperature range being investigated. Since silicon is a semi-transparent material, the emissivity of the heater block can also affect the measured emissivity. As such, in these experiments the measured emissivity was that of a conglomeration of emitters constituting the heater block, the substrate and the PC lattice. At the end the question remains: how does the reflectance of the photonic crystal-substrate system relate to the inherent reflectivity of a free-standing photonic crystal?

In this paper we report on our high-temperature photonic crystal emissivity measurements, and derive the expression for the emissivity of a photonic crystal-substrate system in terms of the separate photonic crystal and

substrate emissivities, and the photonic crystal reflectance based on an "*extended*" Kirchhoff's law. The detailed measurement methodology, and a comparison with a theoretical calculation, is presented.

Emissivity of combined photonic crystal-substrate system

A photonic crystal supported by a substrate allows for convenient handling of the photonic crystal. However, the substrate effect is often not considered in theoretical calculations of the reflectivity and transmissivity. In this case, a tungsten photonic crystal is built on top of a partially-transparent silicon substrate with an unpolished backside. The light scattering effect from the backside of the substrate, and the partial transparency of the substrate itself, introduce tremendous complications in modeling the transmission and reflection of the system [16, 17]. For a uniform semi-transparent material, the emissivity is expressed in terms of reflectivity and transmissivity [17]. In principle one can obtain the emissivity by measuring the reflectivity and transmissivity of the object; this is called an indirect measure (not to be confused with indirect method in the theoretical approaches). To measure the total reflectance and transmittance of a highly scattered object, an integrating sphere is needed [18]. If the sample also needs to be in vacuum to avoid oxidation, this method becomes impractical. Furthermore, this method is incompatible with measuring angular-dependent emission. Therefore, we chose to measure the emission from the sample directly, and obtain the emittance by comparing the emission from a reference object with known emissivity; this is called the direct method. A common method of heating the sample is by clamping it to a solid, heated block, to achieve an isothermal condition with the block, itself. The temperature of the sample surface is determined by comparison to a characterized reference sample mounted next to the sample under test. However, when a sample is attached directly on top of a solid block it introduces an emitter additional to the photonic crystal and the substrate. Therefore, we chose to heat the sample from the edge, but the inevitable temperature profile across the photonic crystal presents a serious challenge to determining the photonic crystal temperature. In the later part of this paper, we will describe, in detail, the methodology of how this challenge was met and mitigated.

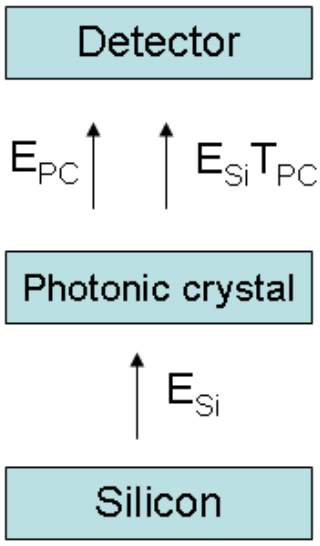

Figure 1: Independent emitter model for the photonic crystal-substrate system emission.

To determine the emissivity of the photonic crystal-substrate system, we consider the photonic crystal and the substrate as two

independent isothermal emitters, as shown in Figure 1. For the moment we consider the perturbation posed by having one side of the photonic crystal in contact with the silicon substrate to be small allowing their treatment as independent emitters. Later we will show that our experimental results support this model. In this independent emitter model, the effective emission is the sum of the emission from the photonic crystal and the transmitted emission from the silicon substrate. In terms of the effective emissivity (E_{eff}), it is expressed as,

$$E_{eff} = E_{PC} + E_{Si} * T_{PC} = (1 - R_{PC}) + (E_{Si} - 1) * T_{PC}, \quad (1)$$

where R_{PC} and T_{PC} are the total reflectivity and transmissivity of the free-standing photonic crystal, respectively, E_{PC} and E_{Si} are the emissivity of the

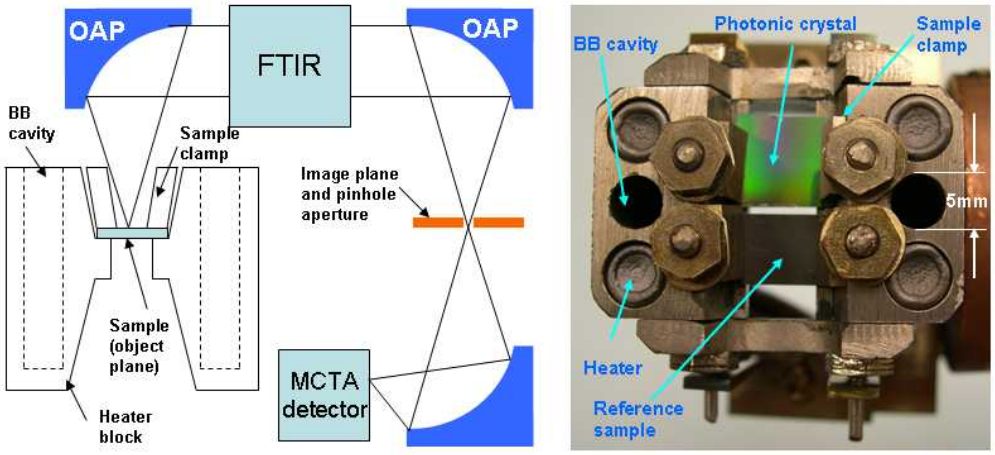

Figure 2: Optical system and heater block of the emission experiment. The picture on the right shows the photonic crystal and reference samples mounted next to each other.

photonic crystal and silicon substrate respectively. If the silicon substrate is replaced with a blackbody substrate, equation (1) reduces to the photonic crystal emissivity 1-R_{PC}. On the other hand, if E_{Si} is zero, which is the room temperature case, the E_{eff} is just the absorptivity of the photonic crystal. Therefore, by measuring separately the emissivity of the silicon substrate and the photonic crystal-substrate system, we can accurately validate the theoretical prediction of the total reflectivity and transissivity of the photonic crystal itself. The importance of this equation is that we do not have to measure the total transmittance and reflectance of the substrate or the photonic crystal.

Experimental method and calibration

The main challenges to any emissivity measurement are: determining the temperature of the sample, and the calibration of the detector gain and spectral response. In addition, stray light entering into the detection system can also introduce error. In this section, we will describe the optical system and calibration procedures used to perform our emissivity measurements. The

schematic diagram of the apparatus is shown in Figure 2. An off-axis parabolic mirror (152 mm focal length) is used to collect (full collection angle of 19°) and relay image the emission from the sample to an image plane, where an approximately 1.5 mm diameter aperture is placed. The transmitted light is collected and focused by another off-axis parabolic mirror into a mercury cadmium telluride (MCT) detector. The image plane is located in the sample chamber of the FTIR (Fourier Transform Infrared) spectrometer (a Nicolet Nexus 870 with a CaF_2 beamsplitter). The imaging system has a demonstrated 0.5 mm resolution, consistent with the size of the pinhole used. The vacuum Dewar that houses the sample-heater block system is on an x-y translation stage to allow emission measurements to be made on one of the two samples, the blackbody cavities, or any part of the heater block. The imaging system and the fixed aperture maintain a constant sampling area from the sample, and keep stray light from entering into the detector. A background light level without any sample scattered in the vacuum dewar on the order of 1% of the signal from the blackbody cavity. Because the silicon substrate has an emissivity of about 0.7-0.8 at elevated temperatures, this contribution is reduced to 0.3% which far less than other sources of uncertainty.

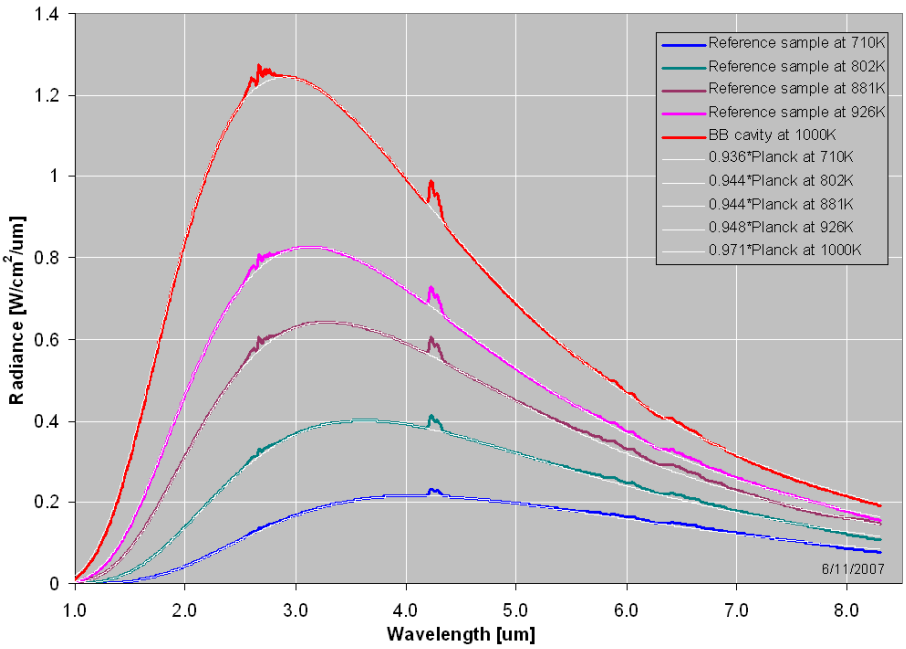

Figure 3: Emission from the reference sample at several temperatures, and the left blackbody cavity in the heater block at 1000K. The fitted Planck distribution curves (dashed) are overlaid on top of these curves. The emissivity factor of each curve is shown in the legend. The features that protrude out of the Planck curve are due to small difference in the water absorption from the calibration beam path.

The sample is heated conductively by the heater block from two sides of the sample, as shown in Figure 2. Every component of the heater block, including sample clamps, nuts, washers and threaded rods are made of molybdenum, which remove mismatches in thermal expansion coefficients. The molybdenum construction also allows the sample to be heated to temperatures substantially beyond 1000 K. Four cylindrical heater cartridges from Watlow (Firerod E1A51-9505) can deliver up to 450W of total power to the block. In the experiments we report here, a total input power of about 100W was used to achieve a heater block temperature of 1000 K.

The heater block has two built-in cylindrical blackbody cavities, each 23 mm deep with a 5 mm diameter. The cavities are coated with high-temperature Aremco HiE840 paint, producing an effective emissivity of 0.97, as measured with the focal plane 6.3 mm into the hole. This effective emissivity is consistent with the calculations by Chandos [19]. Emissions from these cavities are used to determine the heater block temperature, provide an *in situ* emissivity calibration, and serve as a convenient position marker for mapping the temperature profile of the reference and sample under test (SUT). Upon correcting the FTIR-detector system response using a NIST-traceable blackbody source, the temperature of the blackbody cavity in the heater block can be determined to within +/-0.7 K.

Two samples can be mounted on the heater block with independent clamps. One of these samples serves as a reference sample, and the other is the SUT. The reference sample will be used to determine the temperature of the SUT. Because the samples are heated from two ends, they have a parabolic-like temperature profile between the two heat sources. At the center, the temperature gradient is at a minimum at the coldest part of the sample, and is therefore the location at which the emission measurement is taken. Because our sampling spot size is 2mm dia, the measured temperature is an average temperature of the sample over this area. Based on finite element thermal analysis, the average temperature over a 2 mm region where the temperature gradient is at a minimum is 0.07% higher than the temperature at the minimum point. This error is small, even compared with the temperature uncertainty of the NIST-traceable blackbody source.

In order to determine the temperature of the sample under test, we use the temperature of the reference sample as our thermometer. The reference sample is a piece of silicon with the same thickness as the photonic crystal substrate. It has the same temperature profile as the SUT, due to them having the same heat transfer properties. To ensure the reference sample has a temperature- and wavelength-independent emissivity, a thin film of nitrogen-poor aluminum nitride with a dark-grey matte finish was deposited on the polished side of the silicon surface; this coating is referred as MDL black. Upon coating the MDL black with HiE840 black paint, the material has a stable emissivity of 0.94 +/-0.014 under repeated temperature and vacuum

cycling. By replacing the sample under test with a second reference sample, and mapping the temperature along the symmetry line, a small temperature variation caused by the differences in the heater resistances was found. The measured temperature uncertainty at the SUT location is +/-0.3%, and is consistent with our ability to reproducibly position the sample to +/-0.25 mm. At the moment this is the biggest source of error in our emissivity measurements. We believe by controlling the heater voltages independently, this temperature variation on the heater block can be reduced substantially.

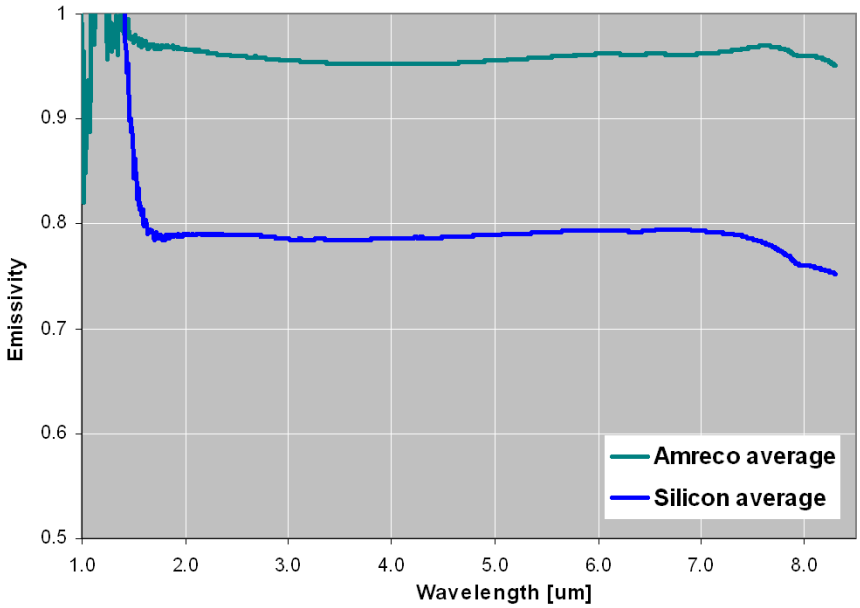

Figure 4: Emissivty of the Aremco paint and the silicon wafer. The silicon sample is 680µm thick, with an unpolished backside and a resistivity of 0.004 - 0.04 Ω-cm.

Detector calibration

Detector spectral and nonlinear gain responses are calibrated using a NIST-traceable blackbody source. This is accomplished by rotating the first off-axis parabolic mirror by 90° to collect the light from the blackbody source. To account for the surface reflection loss, and a small amount of water content in the CaF_2 window, this calibration is performed with the exact same window in the beam path. A family of detector response curves is derived by measuring the blackbody source from 493 to 1183K in intervals of 50-30 K. At temperatures not covered by these measurements, a linear interpolation of the two nearest temperatures is used. Figure 3 illustrates the validity of this calibration method by comparing the corrected detector signals to a calculated Planck spectrum. The temperature uncertainty of the source in the temperature range of 420-960 K is 1.5-1.7 K. This represents an emissivity uncertainty of +/-0.004 in the 3 µm region. To ensure that all the nonlinear responses have

been corrected, we also have to use a nonlinear correction method. The method involves fitting the detector response to a third-order polynomial for each wavelength. These fits have less than one part in 10^4 rms error. The true irradiance from the sample is obtained by finding roots of the cubic equation for each specific wavelength. Experimentally, the measured +/-0.014 emissivity uncertainty from our built-in blackbody cavity is consistent with the estimated uncertainty from this analysis. However, the temperature uncertainty of the sample due to positioning error, and with respect to the reference sample, is +/-0.3%. A summary of the error contributions is shown in Table 1. Assuming these errors are not correlated, the resulting uncertainty in the emissivity at 3 μm is +/- 0.02. Finally, we determine the emissivity of the blackbody cavity in the heater block to be 0.97+/-0.014, and the reference sample is 0.94+/-0.02.

Source	Uncertainty (%)
NIST traceable BB source	±0.4
Detector stability	±1.5
Measurement location	±0.3
Temp difference between reference and test sample	±1.4
Total RMS error	±2.0

Table 1: Error contributions from calibrated source, detector, measurement location and temperature uncertainty of the test sample.

Results and discussions

In order to be able to use the reference sample as the temperature monitor for the SUT, it is important that the emissivity of this material be wavelength-independent and stable over time. The emissivity of the reference sample has been measured many times with vacuum and temperature cycling, and there is no noticeable systematic drift in the emissivity value of the reference sample. The spectral dependence of the emissivity of the reference sample is very flat, as shown in Figure 4. In the spectral region of 1 to 1.5 μm, the data is not trust worthy because of the poor sensitivity of the MCT detector, which hampers the ability to obtain an accurate correction in this region. The silicon emissivity is also found to be temperature- and wavelength-independent for temperatures of 700-960 K. The silicon sample is an n-type <100> surface with a resistivity value of 0.004-0.04 Ω-cm. The emissivity measured is 0.77+/-0.02, a value slightly higher than the 0.69 reported by Sato and Timan [18, 16, 20, 21]. Sato's samples were polished on both sides. Vandenabeele used a silicon wafer 675 μm thick with varying

degrees of roughness on the backside; he measured saturated emissivities of 0.70-0.78 for the different roughnesses [20]. The emissivity of silicon increases with roughness and oxide thickness. Our result is within the range of emissivities one expects from roughened silicon and lends confidence to our measurement methodology. The temperature at which the silicon emissivity saturates is consistent with low resistivity silicon.

The photonic crystal we measured is an 8-layer tungsten logpile photonic crystal with a periodicity of 2.85 µm. The rod width is 0.8 µm, with a height of 1.3 µm. The lowest photonic crystal bandedge occurs at 4.5 µm. The fabrication process [22] and the optical properties of metallic photonic crystals [23] have been discussed in previous publications. If the photonic crystal is free-standing and is heated by a blackbody substrate, then the emissivity is given by 1-R from Eq. 1, which is shown as the brown curve in Figure 5. The broad peak that spans from 2.8 to 3.4 µm, and the features at 4.16 and 4.48 µm, are the propagating modes of the photonic crystal. However, because of the presence of a semi-transparent substrate, the

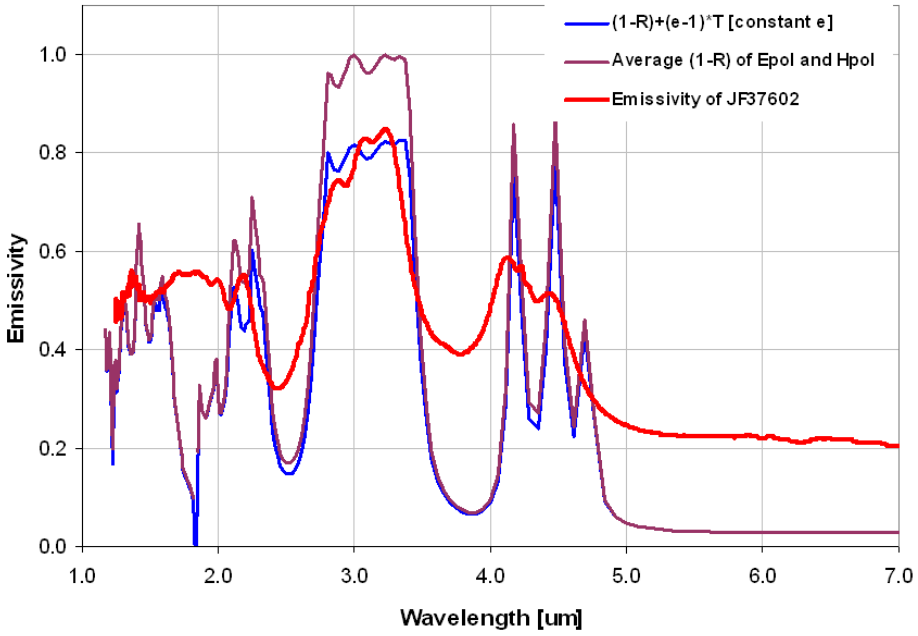

Figure 5: Measured emissivity of photonic crystal is compared with independent emitter model. The red trace is the measured emissivity from the photonic crystal-silicon system. The brown curve is the calculated 1-R, where R is the total reflectivity. The blue curve is the calculated (1-R)+(e-1)*T, where e is the emissivity of the silicon, and R and T are the calculated total reflectivity and transmissivity of the photonic crystal. Since the measured emissivity (0.77) of Si very flat in the wavelength region of interest, a constant value of 0.77 was used.

emissivity is modified and is given by Eq. 1, according to the independent emitter model. The R and T in Eq. 1 are the calculated total reflectivity and

transmissivity of the free standing photonic crystal. For the silicon emissivity we used the measured value of 0.77. This result is shown by the blue curve in Fig. 5, using the measured Si emissivity. This model agrees very well with the measured emissivity of the photonic crystal-substrate system (red curve in Fig. 5). On the other hand, if the substrate emissivity is assumed 1 (brown curve), the disagreement is very significant (25%).

The deep intensity modulation and sharp features at 4.16 μm and 4.5 μm are only qualitatively reproduced in the experimental measurements. This discrepancy may be due to the angular averaging effect over the full acceptance angle of 19^{o} in our measurements. In addition, fabrication imperfections of the photonic crystal, such as variations in the layer thicknesses, rod dimensions and periodicity may also have some contribution. In the temperature range we investigated, we found no significant temperature dependence in the emissivity. We have measured two other samples from the same wafer, while the overall features are the same there are some subtle difference in spectral details and the depth of modulation. This is believed to be due to non-uniformities in the layer thicknesses across the wafer caused by the chemical mechanical polishing process. None of the three samples we measured showed any indication of the non-equilibrium behavior that Chow predicted [8]. Finally, we wish to point out that in reality, the photonic crystal is built on a very thin layer (800 nm) of non-stoichiometric silicon nitride on the surface of the Si, which is required to bond the W rod to the Si wafer; we believe this effect to be small enough so as not to affect the general conclusions of our measurements. Future investigations will attempt to account for the perturbation introduced by this layer. We believe this work represents the most accurate measure of the photonic crystal emissivity with a maximum uncertainty of +/-0.02.

Summary

In summary, we have developed a methodology to measure and model the emissivity of a photonic crystal-substrate system. The relationship between the measured emissivity of the photonic crystal-substrate system and the individual emissivities of the photonic crystal and the substrate is derived and validated. These measurements also show no indication of non-equilibrium behavior.

References

[1] Joannopoulos J.D., Meade R.D. and Winn J.N., *Photonic Crystals,* Princeton University Press, Princeton, 1995.

[2] Lin S.Y., Fleming J.G., and El-Kady I., "Three-dimensional photonic-crystal emission through thermal excitation", *Opt. Lett.*, **28**, 1909 (2003).

[3] Lin S.Y., Moreno J., Fleming J.G., "Three-dimensional photonic-crystal emitter for thermal photovoltaic power generation", *Appl. Phys. Lett.*, **83**, 380 (2003).
[4] Lin S.Y., Fleming J.G. and El-Kady, I, "Highly efficient light emission at λ=1.5 μm by a three-dimensional tungsten photonic crystal", *Opt. Lett.*, **28**, 1683 (2003).
[5] Cornelius C.M. and Dowling J.P., "Modification of Planck blackbody radiation by photonic band-gap structures", *Phys. Rev. A*, **59**, 4736 (1999).
[6] Florescu M., Busch K., Dowling J.P., "Thermal radiation in photonic crystals", *Phys. Rev. B*, **75**, 201101(R), (2007).
[7] El-Kady I., Chow W.W. and Fleming J.G., "Emission from an active photonic crystal", *Phys. Rev. B*, **72**, 195110 (2005).
[8] Chow W.W., "Theory of emission from an active photonic lattice", *Phys. Rev. A*, **73**, 013821 (2006).
[9] Luo C., Narayanaswamy A., Chen G. and Joannopoulos J.D., "Thermal Radiation from Photonic Crystals: A Direct Calculation", *Phys. Rev. Lett.*, **93**, 2139051 (2004).
[10] Chan D.L.C., Soljacic M. and Joannopoulos J.D., "Direct calculation of thermal emission for three-dimensionally periodic photonic crystal slabs", *Phys. Rev. E*, 74, 036615 (2006).
[11] Snyder W.C., Wan Z. and Li X., "Thermodynamic constraints on reflectance reciprocity and Kirchhoff's law", *Appl. Opt.*, 74, 3464 (1998).
[12] Trupke T., Wurfel P., and Green M.A., "Comment on ''Three-dimensional photonic-crystal emitter for thermal photovoltaic power generation", *Appl. Phys. Lett.*, **84**, 1997 (2004).
[13] Greffet J.J., Nieto-Vesperinas M., "Field theory for generalized bidirectional reflectivity: derivation of Helmholtz's reciprocity principle and Kirchhoff's law", *J. Opt. Soc. Am. A*, **15**, 2735 (1998).
[14] Lin S.Y., Moreno J., and Fleming J.G., "Response to ''Comment on Three-dimensional photonic-crystal emitter for thermal photovoltaic power generation' '' .Appl. Phys. Lett. 84, 1997 .2004.. *", Appl. Phys. Lett.*, **84**, 1999 (2004).
[15] Seager C.H., Sinclair M.B., and Fleming J.G., "Accurate measurements of thermal radiation from a tungsten photonic lattice", *Appl. Phys. Lett.*, **86**, 244105 (2005).
[16] Sato T., "Spectral Emissivity of Silicon", *Jap. J. of Appl. Phys.*, **6**, 339 (1968).
[17] McMahon H.O., "Thermal Radiation from Partially Transparent Reflecting Bodies", *J. of Opt. Soc. Am.*, **40**, 376 (1950).
[18] Chubb D.L., Wolford D.S., Meulenberg A. and DiMatteo R.S., "Semiconductor Silicon as a Selective Emitter", *AIP conference proceedings* **653**, 174 (2003).
[19] Chandos R.J. and Chandos R.E., *Appl. Optics*, **13**, 2142 (1974).

[20] Vandenabeele P. and Maex K., "Influence of temperature and backside roughness on the emissivity of Si wavers during rapid thermal processing", *J. of Appl. Phys.*, **72**, 5867 (1992).
[21] Timan P.J., "Emissivity of silicon at elevated temperatures", *J. of Appl. Phys.*, **74**, 6353 (1993).
[22] Fleming J.G., Lin S.Y., El-Kady I., Biswas R., and Ho K.M., "All-metallic three-dimensional photonic crystals with a large infrared bandgap"**,** *Nature*, **417**, 52 (2002).
[23] Lin S.Y., Fleming J.G., Li , El-Kady I., Biswas R. and Ho K.M., *J. Opt. Soc. Am. B*, **20**, 1538 (2003).

Acknowledgement

The authors would like to acknowledge Mike Skeyka at University of New Mexico for performing the finite element thermal analysis of the sample, and A. R. Ellis for fruitful discussions and assistance in this experimental effort. This work is supported by the LDRD program at the Sandia National Laboratories, a multi-program laboratory operated by Sandia Corporation, a Lockheed Martin Company, for the U.S. Department of Energy's National Nuclear Security Administration under contract DEAC04-94A85000.